MedChemComm

Accepted Manuscript

ROYAL SOCIETY OF CHEMISTRY

www.rsc.org/medchemcomm

Cite this: DOI: 10.1039/c0xx00000x

www.rsc.org/xxxxxx

CONCISE ARTICLE

Design of pyrazolo-pyrimidines as 11β-HSD1 inhibitors through optimisation of molecular electrostatic potential

Graeme R. Robb,*[a] Scott Boyd,[a] Christopher D. Davies,[a] Alexander G. Dossetter,[a] Frederick W. Goldberg,[a] Paul D. Kemmitt,[a] James S. Scott[a] and John G. Swales[a]

Received (in XXX, XXX) Xth XXXXXXXXX 20XX, Accepted Xth XXXXXXXXX 20XX
DOI: 10.1039/b000000x

The inhibition of 11β-hydroxysteroid dehydrogenase type 1 (11β-HSD1) is a potentially attractive mechanism for the treatment of obesity and other elements of the metabolic syndrome. A series of pyrazolo-pyrimidine inhibitors of this enzyme were identified from directed library synthesis. Knowledge of how these compounds bind to the enzyme and the key hydrogen-bonding interactions was used to design further compounds. The hydrogen-bond acceptor strength was calculated from the molecular electrostatic potential using quantum mechanical theory. Compounds were designed to modulate the acceptor strength, thus optimising the potency and other drug-like properties. Compounds with enhanced CNS penetration were designed through further modification of the electrostatic potential and the hydrogen-bond properties.

Introduction

Obesity has been recognised by the World Health Organisation as a global epidemic. It has been estimated that global obesity levels in 2012 were equal in weight to an additional 56 million people of average body mass.[1] It has been proposed that the reduction of intracellular glucocorticoid concentrations is a potential mechanism for the treatment of obesity and metabolic syndrome.[2-5]

11β-hydroxysteroid dehydrogenase type 1 (11β-HSD1) is an NADPH dependent enzyme, principally expressed in the liver, adipose tissue and the brain.[6] It catalyses the conversion of the inactive glucocorticoid hormone cortisone to the active glucocorticoid cortisol and has a key role in regulating intracellular cortisol concentrations.[7] Inhibition of 11β-HSD1 has therefore been proposed as an attractive method of lowering intracellular glucocorticoid concentrations that could have benefits in the treatment of obesity. In addition, 11β-HSD1 is highly expressed in brain regions important for cognition and is increased in animal models of Alzheimer's disease (AD). Transgenic overexpression of 11β-HSD1 in brain exacerbates age-associated cognitive dysfunction, while 11β-HSD1 knockout mice are protected.[8, 9] Proof of concept in an AD setting has been obtained in humans by use of the nonselective prototype 11β-HSD1 inhibitor carbenoxolone.[10]

More than 25 pharmaceutical companies have some interest in 11β-HSD1 as a target, as evidenced by over 250 patent applications.[11-14] Incyte and Merck have reported data on phase II clinical trials.[15-17] Their results indicate only modest reduction in fasting plasma glucose and glycated haemoglobin – key biomarkers for diabetes. These data suggest that only high doses of 11β-HSD1 inhibitors improve glycemic control in humans and do so only to a modest extent.

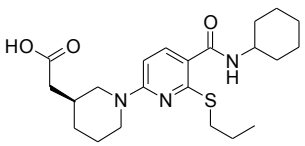

Fig. 1 Compound 1

Researchers at AstraZeneca have previously discovered AZD4017 **1** (Figure 1), an effective inhibitor of 11β-HSD1 in human adipocytes, and selected it for clinical development.[18] Our own experiences in a pre-clinical setting agree with the published clinical data and indicate that only very high exposures of 11β-HSD1 inhibitors provide efficacy. We hypothesised that modest exposure in the central nervous system (CNS) may account for the limited efficacy, despite high exposure in the peripheral tissues.[19] 11β-HSD1 is expressed in areas of the brain relevant to metabolic control,[20] and glucocorticoids are known to have effects on neuropeptides in the hypothalamus, including proopiomelanocortin (POMC) and neuropeptide Y (NPY), which are crucially involved in food intake and have also been shown to control glucose levels via the vagal nerve.[21, 22] One potential risk of inhibiting 11β-HSD1 in the brain is that it may lead to activation of the hypothalamic-pituitary-adrenal (HPA) axis. Initial data from trials have shown some evidence for modest increases in androgens and adrenocorticotropic hormone, consistent with HPA axis activation, but within normal physiological levels.[23] In order to test our hypothesis and assess the potential risks we require compounds capable of reaching and inhibiting 11β-HSD1 in the brain (in addition to peripheral tissues) and thus a back-up program was initiated with the task of discovering 11β-HSD1 inhibitors with good CNS exposure.

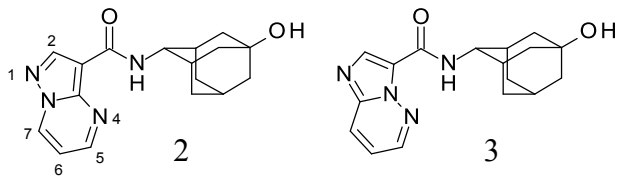

Fig. 2 Compounds 2 and 3. The numbering scheme for pyrazolo-pyrimidine core is also indicated.

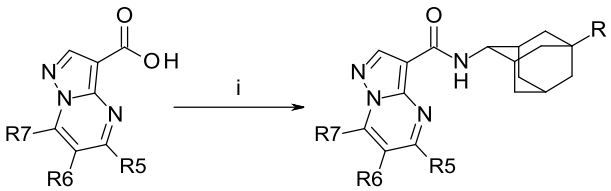

Scheme 1 General synthetic route. Reagents and conditions: (i) amine, HATU, DIPEA, DMF. R = OH, CN, H, OCH_3

Another branch of this work involving a different chemical series has been reported by Goldberg *et al*.[24]

Designing compounds to achieve exposure in the brain is a two-fold challenge: first a drug must have a high permeability at the blood-brain barrier, and secondly the drug must not be a substrate for efflux by one of the many transporters expressed at this membrane. These goals typically require different pharmacokinetic and pharmacological profiles to peripherally acting compounds. Predicting these properties is difficult, however some general principles of CNS drug-design have been derived from an analysis of marketed drugs.[25-27] The general principles for attaining good CNS exposure are that the drug should have (i) a low molecular weight, less than 400 Daltons; (ii) a low polar surface area, less than 90 $Å^2$; (iii) a moderate lipophilicity, $1 < \log D < 3$; (iv) a maximum of one hydrogen-bond donor; and (v) the avoidance of acids. These criteria provided clear design guidelines for our CNS penetrant 11β-HSD1 inhibitor program.

Results and discussion

Through profiling of the acidic compound **1** it was determined that this and similar acidic compounds would have a low likelihood to achieve significant CNS exposure. The desired profile was therefore of a neutral compound from a related series to **1**. Previous work had identified that *N*-(5-hydroxy-2-adamantyl)-amide was a beneficial fragment for use in 11β-HSD1 inhibitors, possessing a good balance of potency, lipophilicity and metabolic stability.[18, 19] Using the structure activity relationships observed with **1** and related compounds, a library was designed where the hydroxy-adamantyl-amide fragment was fixed and the remainder of the molecular structure explored, based upon a focussed reagent selection. The library was screened in an 11β-HSD1 enzyme inhibition assay.

Two of the compounds found from this screen were **2** and **3** (Figure 2), related inhibitors of 11β-HSD1 with IC_{50} values of 0.1 μM and 1.1 μM respectively. These compounds were not considered sufficiently potent to be progressed into further studies, but compound **2** does have an attractively low lipophilicity ($\log D_{7.4}$ = 1.2) and thus a respectable 'ligand lipophilicity efficiency'[28] (LLE = $pIC_{50} - \log D_{7.4}$ = 5.8). One

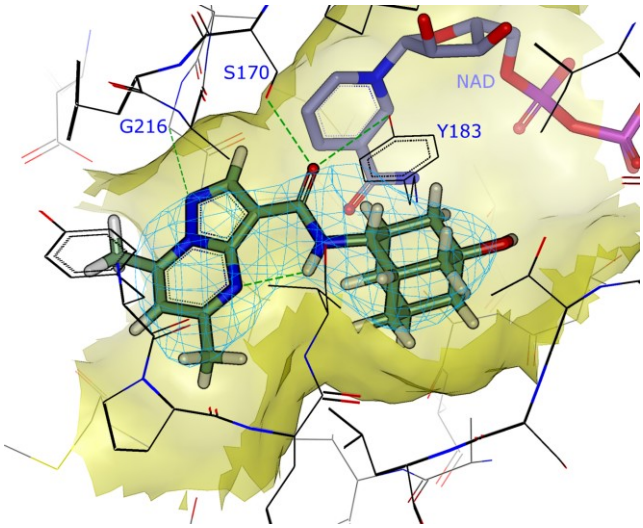

Fig. 3 The structure of compound 7 bound to 11β-HSD1, solved from single crystal X-ray diffraction. The protein surface is shown in gold, the ligand electron-density is shown in blue wireframe. Hydrogen-bonds to S170 and Y183 are indicated.

potential limitation of this compound is that it formally possesses two hydrogen-bond donors, which may limit its CNS exposure. However, it was recognised that the proximity of a hydrogen-bond acceptor (4-position of the aromatic system) would partially mask the effect of one donor, which was felt would increase the likelihood of CNS exposure. Furthermore, the compound is small (MW = 312 Daltons), with a good 'ligand efficiency'[29] (ratio of binding energy to non-hydrogen atoms) and with a relatively low polar surface area (PSA = 79 $Å^2$) making it a suitable lead compound for further optimisation.

Compound Synthesis

Compounds were prepared by coupling either *trans* 4-amino-adamantan-1-ol, *trans* 4-aminoadamantane-1-carbonitrile, adamantan-2-amine, or *trans* 5-methoxyadamantan-2-amine with various pyrazolo-pyrimidine acids, 6-cyano-1-methyl-pyrrolo[3,2-b]pyridine-3-carboxylic acid, or imidazo-pyradazine acid, using *N,N,N′,N′*-tetramethyl-*O*-(7-azabenzotriazol-1-yl)uronium hexafluorophosphate (HATU) in the presence of *N,N*-diisopropylethylamine (DIPEA). Some of the substituents on the pyrazolo-pyrimidine ring were introduced during construction of the bicyclic acids prior to coupling, while others were introduced by functional group interconversion subsequent to the amide formation. An illustrative example is shown below with full details in the supporting information.

Synthesis of **2**, *N*-(*trans* 5-hydroxy-2-adamantyl)pyrazolo[1,5-a]pyrimidine-3-carboxamide was performed as follows. *N,N*-Diisopropylethylamine (0.536 mL, 3 mmol) was added to pyrazolo[1,5-a]pyrimidine-3-carboxylic acid (163 mg, 1.00 mmol), *trans* 4-aminoadamantan-1-ol hydrochloride (204 mg, 1 mmol) and *N,N,N′,N′*-tetramethyl-*O*-(7-azabenzotriazol-1-yl)uronium hexafluorophosphate (457 mg, 1.20 mmol) in *N,N*-dimethylformamide (DMF) (4 mL). The resulting mixture was stirred at ambient temperature for 17 hours. The reaction mixture was diluted with ethyl acetate (25 mL), and washed with water (10 mL). The organic layer was evaporated to afford crude product which was purified by preparative HPLC to afford the

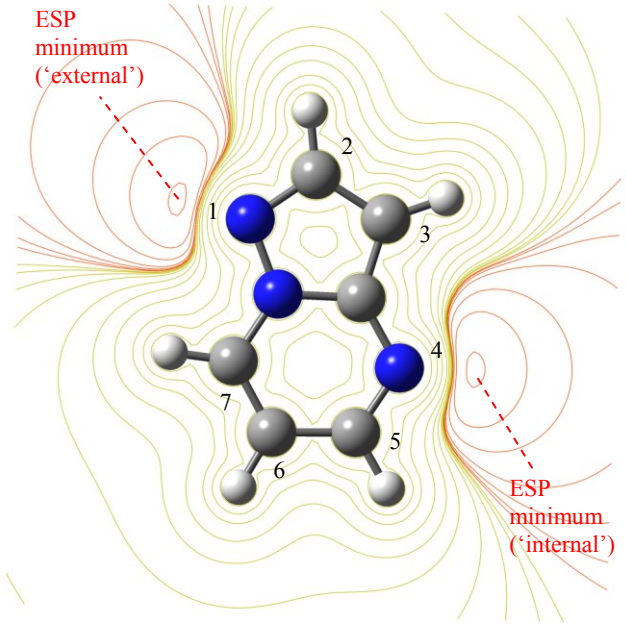

Fig. 4 The calculated electrostatic potential (ESP) associated with a pyrazolo-pyrimidine fragment. Lines indicate isopotential contours, with colouring from red (high ESP) to green (low ESP).

title compound **2** (0.169 g, 54%) as a solid. The compound was characterised by ^{1}H NMR, ^{13}C NMR and mass spectrometry.

Protein-bound conformation

The binding mode of the pyrazolo-pyrimidine series of compounds was predicted from docking and later confirmed using single crystal X-ray diffraction (Figure 3). The protein is refined as a dimer in the asymmetric unit, the ligand binding site being essentially identical for each monomer. The key interactions for potency are a pair of hydrogen-bonds formed from the carbonyl of the ligand to Ser170 and Tyr183. Additionally, from co-crystals of similar compounds, the hydroxyl group of the ligand is known to form interactions with water through to the NADPH cofactor and the protein (see PDB: 4C7K). However, the resolution of the structure was insufficient to resolve solvent molecules in this case.

As predicted, an intermolecular hydrogen-bond is formed between the aromatic nitrogen acceptors at the 4-position of the pyrazolo-pyrimidine ring and the amide NH donor (2.3 Å apart). In addition to promoting the correct conformation for binding, this feature should mask the effect of the donor so that the associated polarity would not be fully exposed at the surface of the molecule. This should increase the likelihood of the compound crossing the blood-brain barrier. One important point to note is that traditional calculated PSA[30] is a rule-based implementation using the 2D molecular scaffold. It is therefore a poor guide in assessing the effect of conformation on the effective polar surface area and was not used to guide design.

Hydrogen-bond acceptor strength

Molecular conformation, though fixed upon binding to the enzyme, is dynamic in solution. The potency of each molecule will therefore partly depend upon the enthalpic penalty in moving from an ensemble of solution conformations to a single bioactive conformation. The presence of an intermolecular hydrogen-bond, as shown in Figure 3 will bias the conformational ensemble towards the bioactive conformation, minimising this penalty. It follows that a stronger hydrogen-bond acceptor at the 4-position will more strongly bias the conformational ensemble towards the bioactive one and thus will result in a more potent compound through an entropic effect. In addition, it is proposed that the more-compact conformation favoured by the formation of the internal hydrogen bond would have a lower surface area, with less exposed polar surface and thus fewer opportunities to interact with the solvent molecules, reducing the enthalpic penalty for desolvation.

The strength of a hydrogen-bond donor (log$k\alpha$) or a hydrogen-bond acceptor (log$k\beta$) may be calculated using quantum mechanics, employing a method described by Kenny.[31, 32] All calculations were performed with Gaussian09,[33] using the restricted Hartree-Fock method, with the 6-31G* basis set. Using this procedure the acceptor strength was derived from the minimum electrostatic potential adjacent to the heteroatom. Figure 4 shows the electrostatic potential around the pyrazolo-pyrimidine unit and the two electrostatic potential minima associated with the two hydrogen-bond acceptors. Note that the calculations were performed on pyrazolo-pyrimidine fragments only, that did not contain the amide or adamantyl groups. This was in order to derive a clear view of the hydrogen-bond acceptor strength without the complicating influence of the amide hydrogen-bond donor convoluting the electrostatic potential.

A second hydrogen-bond acceptor exists at the 1-position of the pyrazolo-pyrimidine ring. The crystal structure (Figure 3) shows that the contact distance (2.7 Å) is correct for a weak CH-X hydrogen-bond, despite the fact that the α-carbon of a glycine residue is not normally associated with hydrogen-bonding characteristics. Here it likely exists as a result of the geometry of the ligand protein-complex rather than being a driving force in its formation. The contribution of this 'external' acceptor to compound potency depends on two competing factors: the free energy gained on making an interaction with the protein, and the free energy used in breaking interactions with water during desolvation. Given the weak nature of CH-X hydrogen-bonds it is expected that in this case increasing the hydrogen bond strength (log$k\beta_{ext}$) will not have a significant effect on the affinity and that increasing the polarity may result in a larger desolvation penalty, hence a net effect of lower potency.

A selection of pyrazolo-pyrimidines was made that attempted to address both of these hydrogen-bonding hypotheses as well as other structure-activity relationship questions. The hydrogen-bond acceptor strengths for the 'internal' hydrogen bond (log$k\beta_{int}$) and the 'external' hydrogen bond (log$k\beta_{ext}$) were calculated across all candidate compounds. The synthesised compounds thus cover a range of hydrogen-bond acceptor strengths.

Hydrogen-bond strength relationships

The potency of these compounds was determined in a human 11β-HSD1 enzyme assay and the log$D_{7.4}$ (in octanol at pH 7.4) was also determined. Table 1 gives details of these measurements and the calculated hydrogen-bond acceptor strengths for 17 compounds. The values are quoted to the appropriate accuracy, taking into account experimental error.

Table 1 The calculated and measured data for a set of related pyrazolo-pyrimidine compounds

Compound	Log$k\beta_{ext}$	Log$k\beta_{int}$	R5[b]	R6[b]	R7[b]	pIC$_{50}$	Log$D_{7.4}$	Solubility (μM)	Rat heps CL$_{int}$ (μL/min/10^{6}cells)
2	1.56	1.49	H	H	H	7.0	1.4	432	3
3[a]	0.54	2.58	H	H	H	6.0	1.2	1020	nv
4	1.64	1.70	CH_3	H	H	7.7	1.9	238	53
5	1.66	1.68	H	CH_3	H	7.2	1.7	124	16
6	1.84	1.42	H	H	CH_3	7.5	2.0	70	nv
7	1.90	1.62	CH_3	H	CH_3	8.2	2.0	99	7
8	1.82	1.46	CH_3	H	CH_2OCH_3	7.6	2.1	40	<2
9	1.20	0.70	CH_3	H	CF_2H	7.6	2.2	130	<2
10	0.98	1.34	CH_3	H	CF_3	7.3	2.3	228	<2
11	0.88	1.11	H	H	CF_3	6.7	2.0	514	7
12	0.85	0.81	cPropyl	H	CF_2H	8.0	2.8	38	9
13	1.69	1.70	CH_2OCH_3	H	CH_3	7.8	1.8	552	<2
14	1.69	1.70	H	CH_2CH_3	H	7.5	2.3	105	29
15	0.92	1.09	H	Cl	H	7.3	1.8	236	10
16	0.41	0.42	H	C≡N	H	6.6	0.6	964	179
17	1.56	1.68	H	OCH_3	H	7.2	1.8	256	11
18	1.84	1.97	H	CH_2CH_2OH	H	6.5	1.0	174	<2

[a] Compound is imidazo-pyridazine, but sufficiently similar to be included in the same analysis.

[b] Substituent numbering follows the standard numbering conventions for pyrazolo-pyrimidine substitution, see Figure 2

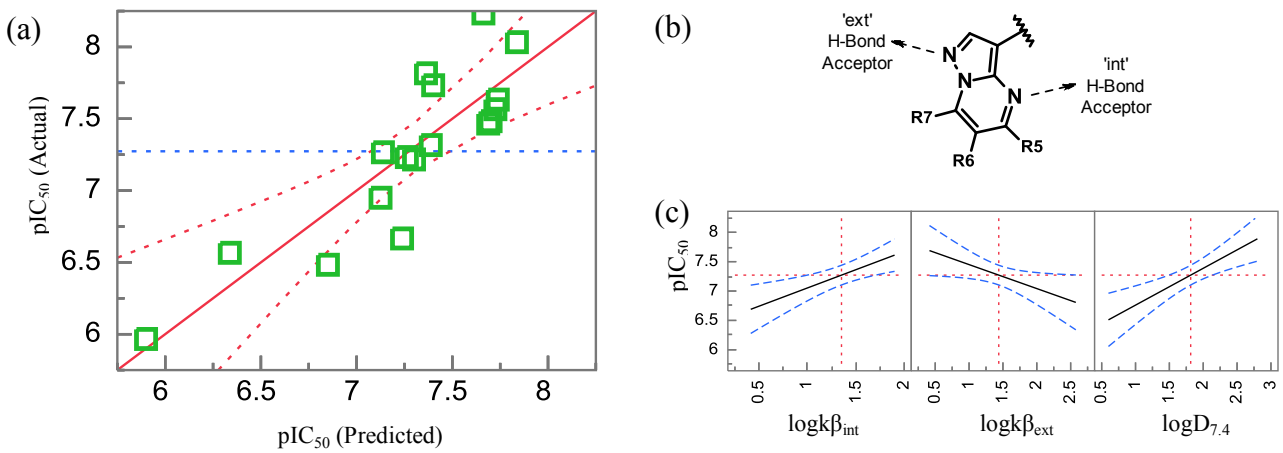

Fig. 5 (a) A model of pIC$_{50}$, predicted from log$k\beta_{int}$, log$k\beta_{ext}$ and log$D_{7.4}$. $R^2 = 0.76$, RMSE = 0.32. (b) the positions of 'internal' and 'external' H-bond acceptors. (c) the variable profile indicating how each variable affects potency.

Using linear regression a simple relationship was derived between potency, the log$k\beta$ values of the two acceptors and the log$D_{7.4}$.

$$pIC_{50} = C + A_1 \log D_{7.4} + A_2 \log k\beta_{int} - A_3 \log k\beta_{ext} \quad (1)$$

The constants in equation (1) are defined: C = 5.87 ± 0.41 (P < 0.0001), A_1 = 0.63 ± 0.16 (P = 0.0018), A_2 = 0.63 ± 0.19 (P = 0.0052), A_3 = 0.41 ± 0.18 (P = 0.038). Note that the probability (P) quoted is for the number being insignificantly different from zero. All variables here are therefore significant. The model is judged to be of a high quality, with the three input variables explaining 76% of the variance (R^2) in potency and a root mean squared error (RMSE) of 0.32 between the predicted and the measured values.

The model shows the expected relationship between hydrogen-bond acceptor strength and potency (Figure 5), *i.e.* as the *internal* hydrogen-bond acceptor increases in strength, the potency also increases and as the *external* hydrogen-bond acceptor increases in strength, the potency decreases. The relationship also includes log$D$ as a factor and this is not unexpected for compounds in the same series. This is largely a consequence of the more hydrophilic compounds requiring more energy to desolvate. It should be noted that there are no significant correlations between log$D$ and log$k\beta_{int}$ or log$k\beta_{ext}$. R^2 values for these correlations are 0.037 and 0.032 respectively.

Solubility (S) of these compounds can also be predicted to a reasonable level of accuracy using only the calculated hydrogen-bond acceptor strengths and the measured log$D$.

$$\log(S/\mu M) = A_1 \log k\beta_{int} + A_2 \log D_{7.4} - A_3 (\log D_{7.4})^2 \quad (2)$$

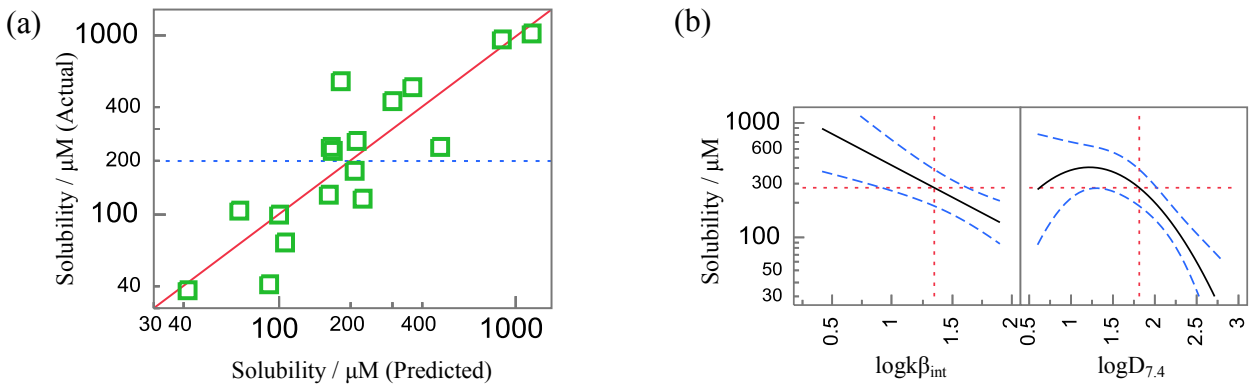

Fig. 6 (a) A model of solubility, predicted from log$k\beta_{int}$ and log$D_{7.4}$. $R^2 = 0.76$, RMSE for log(solubility) = 0.54. (b) the variable profile indicating how each variable affects solubility. Note, $logD_{7.4} < 1$ is not part of the applicability domain.

Table 2 The calculated and measured data for a matched pair of compounds through heteroatom substitution in the aromatic ring

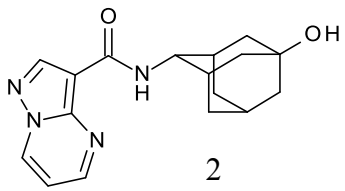

2

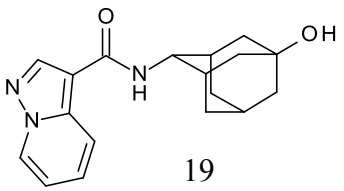

19

Log$k\beta_{int}$	Log$k\beta_{ext}$	pIC$_{50}$	log$D_{7.4}$	Solubility (µM)	Log$k\beta_{int}$	Log$k\beta_{ext}$	pIC$_{50}$	log$D_{7.4}$	Solubility (µM)
1.56	1.49	7.0	1.4	432	na	2.06	6.3	1.5	251

The constants in equation (2) are defined: C = 6.01 ± 0.76 (P < 0.0001), A_1 = 1.28 ± 0.33 (P = 0.0019), A_2 = 2.86 ± 0.28 (P = 0.0002), A_3 = 1.17 ± 0.42 (P = 0.015). The probabilities indicate all variables are significant. The model (Figure 6) is judged to be of a high quality with variables explaining 70% of the variation (R^2) and with a RMSE in prediction of log(solubility) of 0.54 between predicted and measured values.

In the General Solubility Equation (GSE) the solubility can ideally be modelled by the log*D* (a surrogate for the desolvation energy) and the melting point (a surrogate for the lattice-breaking energy).[34] A Log*D* term is present and correct in this model and the presence of the higher order term may be a proxy for the lattice energy. The log$k\beta$ terms might also be expected to contribute to the lattice energy but in this case the strength of the 'external' acceptor does not have a significant effect on the model. The implication is that logD^2 is a better descriptor of the differences in lattice energy and of interactions in the solid state, in this instance. This may indicate a solid form dominated by non-polar contacts rather than hydrogen-bonds. The model *does* show that the solubility decreases with increasing 'internal' hydrogen-bond acceptor strength. This implies that stronger intermolecular hydrogen-bonds in the solid state - and thus a higher desolvation penalty - drive the poor solubility for compounds where log$k\beta_{int}$ is high.

Effect of removal of a hydrogen-bond acceptor

The internal hydrogen bond is clearly important for the potency of these compounds. To test this relationship the reverse hypothesis was investigated, *i.e.* what are the properties of compounds lacking an internal hydrogen bond? The clearest comparison is to replace the pyrimidine nitrogen (4-position) with CH, compound **19**. Table 2 shows a matched pair of compounds[35] exhibiting this change. The transformation results in a significant drop in the potency, which coupled with the essentially static log*D* gives a lower ligand lipophilicity efficiency (LLE) than the parent compound. At face value it may seem somewhat surprising that replacement of an aromatic nitrogen with a carbon has little effect on the log*D*. However, we must consider that the polarity associated with this nitrogen is partially masked by the internal hydrogen bond. Replacement of this nitrogen removes its associated polarity, but also exposes additional polarity due to the hydrogen bond donor of the amide. The net result is no change in the measured lipophilicity.

This result seems to confirm the hypothesis that the internal hydrogen bond is important to help the molecules attain the binding mode conformation. The absence of this internal interaction, though not absolutely detrimental to the potency, does incur an energetic penalty for the molecule to achieve the bioactive conformation, hence the lower observed potency.

Effect of removal of a hydrogen-bond donor

This series of 11β-HSD1 inhibitors possesses two hydrogen-bond donors (albeit one is partially masked). Our hypothesis was that reducing this number would give high brain exposure across the series. The amide donor has historically proven to be difficult to replace without losing potency, *e.g.* simply methylating the amide

Table 3 The calculated and measured data of several sets of matched pairs by substitution at the 5-position of the adamantyl group

R5	R6	R7	5' group	Compound	pIC_{50}	Log$D_{7.4}$	Solubility (μM)	Rat heps CL_{int} (μL/min/10^6cells)	Hu MDCK apparent permeability (10^{-6}cm/s)	Hu MDCK efflux ratio	Total Brain-Blood Ratio[a]	Free Brain-Blood Ratio[b]
H	H	H	OH	2	7.0	1.4	432	3	-	-	-	-
			H	20	7.9	3.5	12	68	-	-	-	-
CH_2OCH_3	H	CH_3	OH	13	7.8	1.8	552	2	-	-	-	-
			C≡N	21	7.7	2.4	54	24	-	-	-	-
H	CH_3	H	OH	5	7.2	1.7	124	16	29	0.8	0.3	0.3
			C≡N	22	7.2	2.3	45	42	46	0.5	1.6	1.0
			OCH_3	23	7.3	2.6	181	14	49	0.5	NV[c]	NV[c]
H	H	CH_3	OH	6	7.5	2.0	70	-	-	-	0.3	0.3
			C≡N	24	7.6	2.4	117	124	-	-	-	-
CH_3	H	CH_3	OH	7	8.2	2.0	99	7	-	-	-	-
			C≡N	25	8.0	2.9	7	107	-	-	-	-
CH_3	H	CH_2OCH_3	OH	8	7.6	2.1	40	2	-	-	-	-
			C≡N	26	7.8	2.7	-	2	-	-	-	-
H	Cl	H	OH	15	7.3	1.8	236	10	44	0.5	0.3	0.4
			C≡N	27	7.2	2.5	44	17	41	0.5	0.6	0.9
H	CH_2CH_2OH	H	OH	18	6.5	1.0	174	2	-	-	-	-
			C≡N	28	6.4	1.6	41	67	-	-	-	-

[a] The Total Brain-Blood Ratio is the ratio of the measured concentrations of the molecule in brain and in whole blood as measured in Han Wistar rats, one hour after dosing.

[b] The Free Brain-Blood Ratio is the ratio of measured free concentration of the molecule in brain (corrected for binding to rat brain tissue) and in blood (corrected for binding to rat serum protein).

[c] The measured levels in both blood and brain were below the minimum level of quantification.

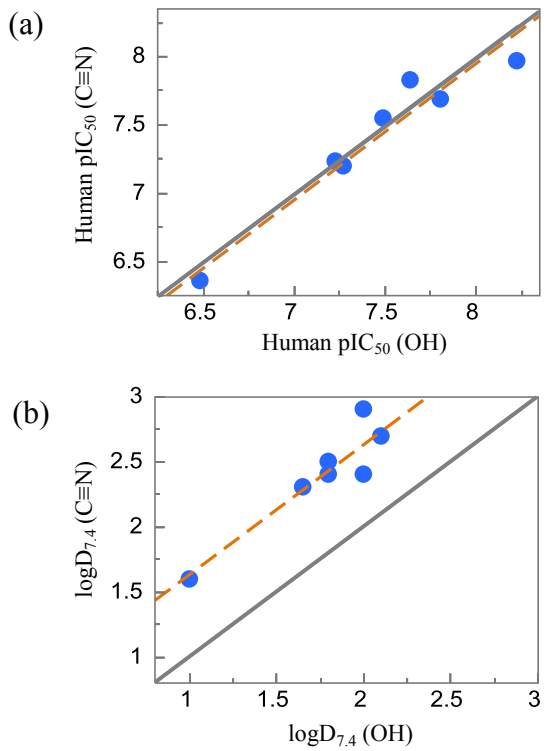

Fig. 7 Molecular-matched pairs of compounds containing either hydroxy or cyano adamantyl, showing (a) pIC_{50} and (b) $logD_{7.4}$. Properties for cyano-containing compounds are on the Y-axis; hydroxyl-containing compounds on the X-axis. 1:1 line in grey and mean change in the property indicated in orange (dashed).

of related active compounds loses all enzyme activity (data not shown). Instead we looked at removal of the donor from the hydroxy group.

The previous structure variations had kept the 5-hydroxy-2-adamantyl group constant. The design challenge was to find a replacement for the hydroxyl that would not significantly erode the solubility and metabolic stability. Table 3 shows compounds **2** and **20**, a matched molecular pair where the hydroxyl group has been removed. Although the inhibition potency has increased by an order of magnitude, the lipophilicity has increased beyond acceptable limits and the LLE is reduced as a result. Furthermore the solubility has dropped sharply following this change and the extent of metabolism has risen, both in keeping with the log*D* increase.

Compounds **5** and **23** show another molecular matched pair where the hydroxyl has been replaced, this time with methoxy (table 3). The data for the methoxy compound look promising: the potency, solubility and *in vitro* metabolism have all been maintained and, while the lipophilicity has increased, it is within acceptable limits. This compound was progressed to *in vivo* studies. However, the observed *in vivo* metabolism of compound **23** was much greater than expected with an *in vivo* clearance of 100 mL/min/kg (apparently greater than liver blood flow) and a fraction absorbed of only 3% (*c.f.* a clearance of 28 mL/min/kg and a fraction absorbed of 32% for its partner, compound **5**). No compound was detected in the CNS. The methoxy group was therefore deemed an unsuitable replacement for the hydroxyl.

A third strategy was the replacement of the hydroxyl group with a cyano group. This group is predicted to be able to make

hydrogen-bonding interactions with solvent molecules in the ligand binding site, similar to those existing for the hydroxyl. Table 3 shows seven matched molecular pairs where this change has been made. Across these examples the inhibition potency has been maintained (mean ΔpIC_{50} = -0.05 ± 0.14) and the log*D* has increased (mean $\Delta \log D_{7.4}$ = 0.64 ± 0.15), see Figure 7. The log*D* increase is undesirable, but tolerated given the greater potential for CNS penetration for removing the hydrogen bond donor. The trend with solubility (mean Δlog(solubility) = -0.62 ± 0.48) and *in vitro* clearance (mean $\Delta \log(CL_{int})$ = 0.73 ± 0.61) are less clear due to the wide range of results observed.

A common and useful means of assessing the likely permeability at the blood-brain barrier is through an *in vitro,* human MDCK transporter assay, measuring both the apparent permeability and the efflux ratio. Several compounds were tested in this assay (table 3) and the results indicate that all tested compounds are highly permeable and have a low efflux liability. Given the lack of useful differentiation observed, we decided to use *in vivo* CNS penetration studies as a means of further assessing blood-brain barrier permeability.

Two cyano-containing compounds with low *in vitro* metabolism values were advanced into *in vivo* CNS-penetration studies. Examining the matched-pairs for these compounds in table 3 reveals that the ratio of free compound in the brain to free compound in the blood has increased in both cases; for compound **22** the ratio is 1.0 making this the first compound in this series to be identified with equal exposure in the brain and periphery.

Ultimately this CNS penetrant compound successfully follows the general design rules for CNS drugs. It is a neutral compound, the molecular weight has been kept low (335 Daltons), the polar surface area has been maintained relative to the starting point (75 $Å^2$ using the rule-based, conformationally naive method), the lipophilicity has been maintained in the correct range ($\log D_{7.4}$ = 2.3) and there is only one (masked) hydrogen bond donor.

Compound **22** was duly selected for further profiling in *in vivo* efficacy studies in a diet-induced obese mouse model. However, this study was cancelled as shortly after this (as previously reported by Goldberg *et al*.[24]) profiling of a compound from another series of 11β-HSD1 inhibitors with similarly high CNS exposure failed to support the theory that body-weight effect were centrally mediated. The hypothesis having been disproven, the project was halted.

Conclusions

The principle of designing compounds based on the accurately predicted electronic properties of molecules is an attractive proposition for lead optimisation. It is a rational design process and allows the exploration of the structure activity relationships without significantly increasing the molecular size or complexity, with relatively few compounds making for an extremely rapid and efficient lead optimisation campaign.

This work has demonstrated that, for a series of pyrazolo-pyrimidine-containing compounds, a clear relationship between hydrogen-bond acceptor strength and potency exists. In these compounds a strong hydrogen bond acceptor, capable of forming an internal hydrogen-bond, favours the bioactive conformation, reduces the entropy penalty for conformational adjustment and thus results in more potent inhibitors of 11β-HSD1. Similarly, a strong, externally directed hydrogen-bond acceptor shows reduced potency against 11β-HSD1. This is hypothesised to be a result of increased energy of desolvation without a corresponding increase in the binding affinity to the enzyme. Finally, we reduced the number of hydrogen-bond donors in the molecule by replacing the 5-hydroxy-2-adamantyl group with 5-cyano-2-adamantyl, giving an equivalent potency and metabolic stability but with a higher brain exposure, and in so doing identified a tool compound suitable for further studies.

Acknowledgements

The authors would like to thank Gisela Brändén, for solving the crystal structure used in this work, and Derek Ogg for additional crystallography support..

Notes and References

[a] *AstraZeneca, Alderley Park, Macclesfield, United Kingdom. Tel: +44 1625 515390; E-mail: graeme.robb@astrazeneca.com*

† Electronic Supplementary Information (ESI) available: [details of any supplementary information available should be included here]. See DOI: 10.1039/b000000x/

1. Walpole, S. C.; Prieto-Merino, D.; Edwards, P.; Cleland, J.; Stevens, G.; Roberts, I. The weight of nations: an estimation of adult human biomass. *BMC Public Health*, 2012, **12**, 439.
2. Thieringer, R.; Hermanowski-Vosatka, A. Inhibition of 11β-HSD1 as a novel treatment for the metabolic syndrome: do glucocorticoids play a role? *Expert Rev. Cardiovasc. Ther.*, 2005, **3**, 911-924.
3. Bjorntorp, P.; Holm, G.; Rosmond, R. Hypothalamic arousal, insulin resistance and Type 2 diabetes mellitus. *Diabet. Med.*, 1999, **16**, 373-83.
4. Walker, B. R. Glucocorticoids and cardiovascular disease. *Eur. J. Endocrinol.*, 2007, **157**, 545-559.
5. Tomlinson, J. W.; Walker, E. A.; Bujalska, I. J.; Draper, N.; Lavery, G. G.; Cooper, M. S.; Hewison, M.; Stewart, P. M. 11β-hydroxysteroid dehydrogenase type 1: A tissue-specific regulator of glucocorticoid response. *Endocr. Rev.*, 2004, **25**, 831-866.
6. Edwards, C. R. W.; Benediktsson, R.; Lindsay, R. S.; Seckl, J. R. 11β-Hydroxysteroid dehydrogenases: key enzymes in determining tissue-specific glucocorticoid effects. *Steroids*, 1996, **61**, 263-9.
7. Walker, E. A.; Stewart, P. M. 11beta-Hydroxysteroid dehydrogenase: unexpected connections. *Trends Endocrinol. Metab.*, 2003, **14**, 334-339.
8. Yau, J. L. W.; Noble, J.; Kenyon, C. J.; Hibberd, C.; Kotelevtsev, Y.; Mullins, J. J.; Seckl, J. R. Lack of tissue glucocorticoid reactivation in 11β-hydroxysteroid dehydrogenase type 1 knockout mice ameliorates age-related learning impairments. *Proceedings of the National Academy of Sciences*, 2001, **98**, 4716-4721.
9. Holmes, M. C.; Carter, R. N.; Noble, J.; Chitnis, S.; Dutia, A.; Paterson, J. M.; Mullins, J. J.; Seckl, J. R.; Yau, J. L. W. 11β-Hydroxysteroid Dehydrogenase Type 1 Expression Is Increased in the Aged Mouse Hippocampus and Parietal Cortex and Causes Memory Impairments. *The Journal of Neuroscience*, 2010, **30**, 6916-6920.
10. Sandeep, T. C.; Yau, J. L. W.; MacLullich, A. M. J.; Noble, J.; Deary, I. J.; Walker, B. R.; Seckl, J. R. 11β-Hydroxysteroid dehydrogenase inhibition improves cognitive function in healthy elderly men and type 2 diabetics. *Proceedings of the National Academy of Sciences of the United States of America*, 2004, **101**, 6734-6739.
11. Scott, J. S.; Goldberg, F. W.; Turnbull, A. V. Medicinal Chemistry of Inhibitors of 11β-Hydroxysteroid Dehydrogenase Type 1 (11β-HSD1). *J. Med. Chem.*, 2014, **57**, 4466-4486.
12. Webster, S. P.; Pallin, T. D. 11β-Hydroxysteroid dehydrogenase type 1 inhibitors as therapeutic agents. *Expert Opin. Ther. Pat.*, 2007, **17**, 1407-1422.

13. Boyle, C. D.; Kowalski, T. J. 11β-hydroxysteroid dehydrogenase type 1 inhibitors: a review of recent patents. *Expert Opin. Ther. Pat.*, 2009, **19**, 801-825.
14. Morgan, S. A.; Tomlinson, J. W. 11β-Hydroxysteroid dehydrogenase type 1 inhibitors for the treatment of type 2 diabetes. *Expert Opin. Invest. Drugs*, 2010, **19**, 1067-1076.
15. Rosenstock, J.; Banarer, S.; Fonseca, V. A.; Inzucchi, S. E.; Sun, W.; Yao, W.; Hollis, G.; Flores, R.; Levy, R.; Williams, W. V.; Seckl, J. R.; Huber, R.; for the INCB13739-202 Principal Investigators The 11-β-Hydroxysteroid Dehydrogenase Type 1 Inhibitor INCB13739 Improves Hyperglycemia in Patients With Type 2 Diabetes Inadequately Controlled by Metformin Monotherapy. *Diabetes Care*, 2010, **33**, 1516-1522.
16. Bauman, D. R.; Whitehead, A.; Contino, L. C.; Cui, J.; Garcia-Calvo, M.; Gu, X.; Kevin, N.; Ma, X.; Pai, L.; Shah, K.; Shen, X.; Stribling, S.; Zokian, H. J.; Metzger, J.; Shevell, D. E.; Waddell, S. T. Evaluation of selective inhibitors of 11β-HSD1 for the treatment of hypertension. *Bioorg. Med. Chem. Lett.*, 2013, **23**, 3650-3653.
17. Shah, S.; Hermanowski-Vosatka, A.; Gibson, K.; Ruck, R. A.; Jia, G.; Zhang, J.; Hwang, P. M. T.; Ryan, N. W.; Langdon, R. B.; Feig, P. U. Efficacy and safety of the selective 11β-HSD-1 inhibitors MK-0736 and MK-0916 in overweight and obese patients with hypertension. *Journal of the American Society of Hypertension*, 2011, **5**, 166-176.
18. Scott, J. S.; Bowker, S. S.; deSchoolmeester, J.; Gerhardt, S.; Hargreaves, D.; Kilgour, E.; Lloyd, A.; Mayers, R. M.; McCoull, W.; Newcombe, N. J.; Ogg, D.; Packer, M. J.; Rees, A.; Revill, J.; Schofield, P.; Selmi, N.; Swales, J. G.; Whittamore, P. R. O. Discovery of a Potent, Selective, and Orally Bioavailable Acidic 11β-Hydroxysteroid Dehydrogenase Type 1 (11β-HSD1) Inhibitor: Discovery of 2-[(3S)-1-[5-(Cyclohexylcarbamoyl)-6-propylsulfanyl pyridin-2-yl]-3-piperidyl]acetic Acid (AZD4017). *J. Med. Chem.*, 2012, **55**, 5951-5964.
19. Goldberg, F. W.; Leach, A. G.; Scott, J. S.; Snelson, W. L.; Groombridge, S. D.; Donald, C. S.; Bennett, S. N. L.; Bodin, C.; Gutierrez, P. M.; Gyte, A. C. Free-Wilson and Structural Approaches to Co-optimizing Human and Rodent Isoform Potency for 11β-Hydroxysteroid Dehydrogenase Type 1 (11β-HSD1) Inhibitors. *J. Med. Chem.*, 2012, **55**, 10652-10661.
20. Bisschop, P. H.; Dekker, M. J. H. J.; Osterthun, W.; Kwakkel, J.; Anink, J. J.; Boelen, A.; Unmehopa, U. A.; Koper, J. W.; Lamberts, S. W. J.; Stewart, P. M.; Swaab, D. F.; Fliers, E. Expression of 11β-Hydroxysteroid Dehydrogenase Type 1 in the Human Hypothalamus. *J. Neuroendocrinol.*, 2013, **25**, 425-432.
21. Savontaus, E.; Conwell, I. M.; Wardlaw, S. L. Effects of adrenalectomy on AGRP, POMC, NPY and CART gene expression in the basal hypothalamus of fed and fasted rats. *Brain Res.*, 2002, **958**, 130-138.
22. Beaulieu, S.; Gagné, B.; Barden, N. Glucocorticoid Regulation of Proopiomelanocortin Messenger Ribonucleic Acid Content of Rat Hypothalamus. *Molecular Endocrinology*, 1988, **2**, 727-731.
23. Feig, P. U.; Shah, S.; Hermanowski-Vosatka, A.; Plotkin, D.; Springer, M. S.; Donahue, S.; Thach, C.; Klein, E. J.; Lai, E.; Kaufman, K. D. Effects of an 11β-hydroxysteroid dehydrogenase type 1 inhibitor, MK-0916, in patients with type 2 diabetes mellitus and metabolic syndrome. *Diabetes, Obesity and Metabolism*, 2011, **13**, 498-504.
24. Goldberg, F. W.; Dossetter, A. G.; Scott, J. S.; Robb, G. R.; Boyd, S.; Groombridge, S. D.; Kemmitt, P. D.; Sjogren, T.; Gutierrez, P. M.; deSchoolmeester, J.; Swales, J. G.; Turnbull, A. V.; Wild, M. J. Optimization of Brain Penetrant 11β-Hydroxysteroid Dehydrogenase Type I Inhibitors and in Vivo Testing in Diet-Induced Obese Mice. *J. Med. Chem.*, 2014, **57**, 970-986.
25. Van, d. W., Han; Camenisch, G.; Folkers, G.; Chretien, J. R.; Raevsky, O. A. Estimation of blood-brain barrier crossing of drugs using molecular size and shape, and H-bonding descriptors. *J. Drug Targeting*, 1998, **6**, 151-165.
26. Ghose, A. K.; Herbertz, T.; Hudkins, R. L.; Dorsey, B. D.; Mallamo, J. P. Knowledge-Based, Central Nervous System (CNS) Lead Selection and Lead Optimization for CNS Drug Discovery. *ACS Chem. Neurosci.*, 2012, **3**, 50-68.
27. Pajouhesh, H.; Lenz, G. R. Medicinal chemical properties of successful central nervous system drugs. *NeuroRx*, 2005, **2**, 541-53.
28. Leeson, P. D.; Springthorpe, B. The influence of drug-like concepts on decision-making in medicinal chemistry. *Nat. Rev. Drug Discov.*, 2007, **6**, 881-890.
29. Hopkins, A. L.; Groom, C. R.; Alex, A. Ligand efficiency: a useful metric for lead selection. *Drug Discov. Today*, 2004, **9**, 430-431.
30. Ertl, P.; Rohde, B.; Selzer, P. Fast Calculation of Molecular Polar Surface Area as a Sum of Fragment-Based Contributions and Its Application to the Prediction of Drug Transport Properties. *J. Med. Chem.*, 2000, **43**, 3714-3717.
31. Kenny, P. W. Prediction of hydrogen bond basicity from computed molecular electrostatic properties: implications for comparative molecular field analysis. *J. Chem. Soc. , Perkin Trans. 2*, 1994, , 199-202.
32. Kenny, P. W. Hydrogen Bonding, Electrostatic Potential, and Molecular Design. *J. Chem. Inf. Model.*, 2009, **49**, 1234-1244.
33. Frisch, M. J.; Trucks, G. W.; Schlegel, H. B.; Scuseria, G. E.; Robb, M. A.; Cheeseman, J. R.; Scalmani, G.; Barone, V.; Mennucci, B.; Petersson, G. A.; Nakatsuji, H.; Caricato, M.; Li, X.; Hratchian, H. P.; Izmaylov, A. F.; Bloino, J.; Zheng, G.; Sonnenberg, J. L.; Hada, M.; Ehara, M.; Toyota, K.; Fukuda, R.; Hasegawa, J.; Ishida, M.; Nakajima, T.; Honda, Y.; Kitao, O.; Nakai, H.; Vreven, T.; Montgomery Jr., J. A.; Peralta, J. E.; Ogliaro, F.; Bearpark, M.; Heyd, J. J.; Brothers, E.; Kudin, K. N.; Staroverov, V. N.; Keith, T.; Kobayashi, R.; Normand, J.; Raghavachari, K.; Rendell, A.; Burant, J. C.; Iyengar, S. S.; Tomasi, J.; Cossi, M.; Rega, N.; Millam, J. M.; Klene, M.; Knox, J. E.; Cross, J. B.; Bakken, V.; Adamo, C.; Jaramillo, J.; Gomperts, R.; Stratmann, R. E.; Yazyev, O.; Austin, A. J.; Cammi, R.; Pomelli, C.; Ochterski, J. W.; Martin, R. L.; Morokuma, K.; Zakrzewski, V. G.; Voth, G. A.; Salvador, P.; Dannenberg, J. J.; Dapprich, S.; Daniels, A. D.; Farkas, O.; Foresman, J. B.; Ortiz, J. V.; Cioslowski, J.; Fox, D. J. Gaussian 09, Revision B.01. *Gaussian, Inc., Wallingford CT*, 2010, , .
34. Yalkowsky, S. H.; Valvani, S. C. Solubility and partitioning I: Solubility of nonelectrolytes in water. *J. Pharm. Sci.*, 1980, **69**, 912-922.
35. Griffen, E.; Leach, A. G.; Robb, G. R.; Warner, D. J. Matched Molecular Pairs as a Medicinal Chemistry Tool. *J. Med. Chem.*, 2011, **54**, 7739-7750.